Journal of Photochemistry & Photobiology A: Chemistry 376 (2019) 238–246

Contents lists available at ScienceDirect

Journal of Photochemistry & Photobiology A: Chemistry

journal homepage: www.elsevier.com/locate/jphotochem

A closer look into laurdan as a probe to monitor cationic DODAB bilayers

Marcos K. Masukawa[1], Cintia C. Vequi-Suplicy[2], Evandro L. Duarte, M. Teresa Lamy*

Instituto de Física, Universidade de São Paulo, São Paulo, Brazil

ARTICLE INFO

Keywords:
Laurdan
DODAB
Decomposition as a sum of Gaussians
Generalized polarization
Thermal phase transition

ABSTRACT

Laurdan is a fluorescent molecule largely used to probe the lipid packing and hydration of membranes. In phospholipid bilayers that undergo the gel-fluid thermal transition, Laurdan fluorescent band displays a significant red shift upon the transition. However, Laurdan in DODAB bilayers does not show this characteristic shift of the emission band. Hence, the analysis of the membrane fluidity through the so-called Generalized Polarization (GP) cannot be used with DODAB. Nevertheless, both static and time resolved fluorescence attest that the Laurdan fluorescence in DODAB, like in phospholipids, is composed of two emission bands. The emission bands are associated with excited states with different lifetimes, and the relative intensity of the bands is sensitive to the bilayer thermal phase. Analyses were performed by decomposing the emission spectrum into two Gaussian bands and by computing the Decay Associated Spectra (DAS), the latter with time resolved fluorescence. We conclude that Laurdan in DODAB bilayers is in a shallower position as compared with the probe in phospholipids, possibly due to the small DODAB head group. Hence, Laurdan could be a useful probe to monitor interactions at the surface of DODAB bilayers, for instance with genetic material, quite often associated with cationic vesicles in lipoplexes, with broad medical applications.

1. Introduction

In this paper, we characterize and evaluate the viability of the fluorophore Laurdan (6-Dodecanoyl-2-dimethylaminonaphthalene) as a structural probe in vesicles of the cationic lipid DODAB (dioctadecyldimethylammonium bromide), also called DDAB (see Fig. 1).

The probe Laurdan has been extensively used in phospholipid self-organized structures, such as vesicles [1–7], micelles [8], hexagonal phases [9] and bilayer discs [10], due to the changes in its fluorescent spectrum depending on the hydration and fluidity of its environment. For example, when a phospholipid bilayer in the gel phase is heated and transitions to the fluid phase, the emission spectrum of Laurdan shifts from ~ 440 nm to ~ 490 nm [1,7]. Hydration and rigidity of the bilayer can be altered by lipid composition [11–13], addition of drugs to the membrane [14,15] and by temperature and pressure changes [16,17].

More recently, Laurdan was used as a structural probe in synthetic lipids, including the cationic lipids from the DODAX family (X being a counter ion, usually Br^- or Cl^-). Sobral et al. used Laurdan to characterize DODAB/DPPC (1,2-dipalmitoyl-sn-glycero-3-phosphocholine) vesicles [18] and Suga et al. used Laurdan in mixtures of DODAB with fatty acids [19], while similar methodologies where used by Lemp et al. to study the effects of sucrose esters on the structure of DODAC (dioleoyldimethylammonium chloride) vesicles [20].

Particular attention has been given to the structure of cationic vesicles because they are used in a series of biotechnological and biomedical applications. Many applications explore the fact that cationic vesicles can complex with nucleic acids such as DNA and RNA [21–23] and host hydrophobic molecules in the lipid bulk [24]. That turns cationic vesicles into candidates for vaccine adjuvants [25,26], drug transport carriers [27,28] and for non-viral transfectors [29–31].

However, these applications require further structural knowledge of the vesicle and their complexes either with drugs or nucleic acids. As mentioned, Laurdan has already been used to study the structure of cationic vesicles of the DODAX family. But most of the aforementioned studies rely on the assumption that Laurdan would exhibit the emission shift observed in phospholipids. This could be a reasonable assumption, since the shift during phase transition has been observed in a large set of phospholipid bilayers such as those composed of DPPC [2,3], DMPC (1,2-ditetradecanoyl-sn-glycero-3-phosphocholine) [5,10,32], DMPA (1,2-ditetradecanoyl-sn-glycero-3-phosphate) [33,34], DPPG (1,2-dihexadecanoyl-sn-glycero-3-phospho-(1′-rac-glycerol)) [6], DPPS (1,2-dipalmitoyl-sn-glycero-3-phospho-L-serine) [35], and phospholipid

Abbreviations: DAS, Decay Associated Spectra; DSG, Decomposition as a sum of Gaussians; GP, Generalized Polarization

* Corresponding author at: Instituto de Fisica, Universidade de Sao Paulo, Brazil.
E-mail address: mtlamy@if.usp.br (M.T. Lamy).
[1] Present address: Tokyo Institute of Technology, Room 1710, Building J2, Suzukake-dai campus, 4259-J2-36 226-8502, Nagatsuta-cho, Yokohama, Japan.
[2] Present address: Fundacion IMDEA-Nanociencia Cantoblanco, C/ Faraday 9, Madrid, 28049, Spain.

https://doi.org/10.1016/j.jphotochem.2019.03.006
Received 28 December 2018; Received in revised form 4 February 2019; Accepted 5 March 2019
Available online 08 March 2019
1010-6030/

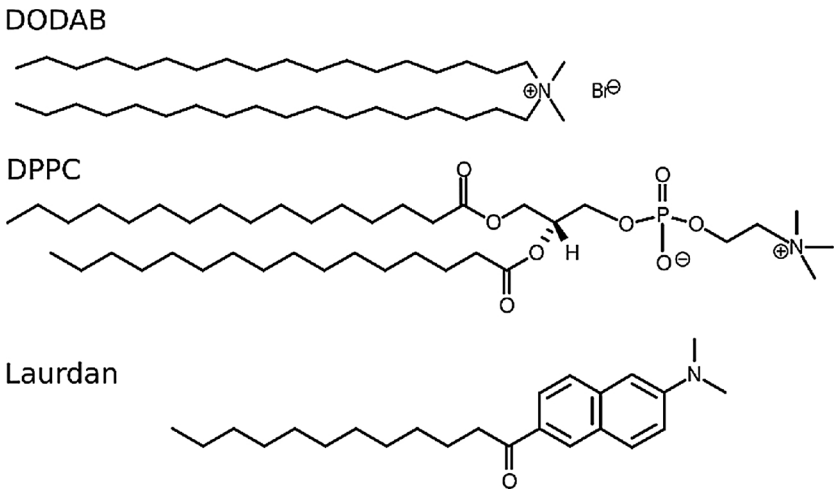

Fig. 1. Molecular structures of DODAB, DPPC and Laurdan.

mixtures [13,15,36–39]. In some of these experiments, researchers performed experiments in a range of pH to test the Laurdan sensitivity to phase transition in phospholipids with neutral, positive and negative charges. For all the phospholipids tested, Laurdan characteristic shift was not affected in the 4–10 pH window [1]. Consequently, the Laurdan spectral shift caused by modifications in the bilayer structure was often taken as an intrinsic behaviour of the probe, and the same analyses of the Laurdan spectra in phospholipids have been used in cationic DODAX vesicles.

To analyse the Laurdan fluorescent spectra, the most usual method has been to calculate the Generalized Polarization (GP). The GP is a normalized difference between the fluorescence intensity at 440 nm and 490 nm, and is defined as [1,7]:

$$GP = (I_{I440} - I_{490})/(I_{440} + I_{490}) \quad (1)$$

where I_{440} is the fluorescence intensity at 440 nm and I_{490} is the fluorescence intensity at 490 nm. Although the intensities can be taken at different positions of the spectra, 440 nm and 490 nm have been ubiquitously used. In phospholipids, positive values for the GP usually mean the bilayer is in the gel phase, and negative values mean the bilayer is in the fluid phase [1,3]. This definition is particularly useful for fluorescent microscopy, because it allows one to estimate the phase of a phospholipid bilayer recording only two wavelengths [40,41].

However, a large amount of information is lost when GP is calculated from the fluorescent spectrum, because only two points from the whole spectrum are considered. While determining the phase of a vesicle using GP works for Laurdan in most phospholipids and phospholipid mixtures, it was shown that for DLPC (1,2-dilauroyl-sn-glycero-3-phosphocholine) vesicles the spectral shift was not caused by phase transition [6].

Another approach for analysing the Laurdan spectrum was based in the observation from time-resolved experiments that Laurdan fluorescence was the emission of actually three excited states [42], two of which can be observed in lipid bilayers. Kozyra et. al suggested that the spectrum could be decomposed as a sum of two Gaussians [43]. Shortly after, the methodology of Laurdan spectrum decomposition was applied and discussed, considering that the population of each state was proportional to the number of photons emitted, that is, to the area under each Gaussian line [6,44]. Accordingly, the phase transition would modify the population of each state, hence changing the shape of the emission spectrum. The spectra decomposition as a sum of Gaussians was validated for Laurdan in DLPC and DPPC vesicles using time-resolved fluorescence, which showed the emission spectra of the excited states were well fit by Gaussian distributions [45]. Here, we use this methodology to study Laurdan fluorescence in DODAB vesicles.

We observed that Laurdan in DODAB vesicles does not show the characteristic emission shift upon gel-fluid transition induced by heating. As we were interested in knowing why Laurdan displays the emission shift in phospholipids but not in DODAB, we comparatively characterized Laurdan in DODAB and DPPC vesicles, with both steady-state and time-resolved fluorescence. The fluorescence spectrum of Laurdan in the two lipids was found to be composed of emissions from at least two excited states, with different lifetimes. However, whereas in DPPC the two excited states display very different energies, in DODAB their energy values were found to be similar. Moreover, fluorescence data indicates that Laurdan in DODAB is at a position with access to more water molecules than the probe in DPPC.

2. Materials and methods

2.1. Materials

DODAB (dioctadecyldimethylammonium bromide) and DPPC (1,2-dipalmitoyl-sn-glycero-3-phosphocholine) were purchased from Avanti Polar Lipids, Inc. (Birmingham, AL, USA). Laurdan (2-dimethylamino-6-lauroylnaphthalene) was from Molecular Probes Inc. (Eugene, OR, USA). HEPES (4-(2-hydroxyethyl)-1-piperazineethanesulfonic acid) was purchased from Sigma Chemical Co. (St. Louis, MO, USA). Milli-Q Plus water was used for buffer preparation.

2.2. Sample preparation

DODAB or DPPC lipid films were formed from chloroform solutions. When used, Laurdan was added to the lipid/chloroform solution in 1 mol% proportion to the lipid content. No Laurdan–Laurdan interaction was found at this probe concentration, as the observed fluorescence spectrum was identical to that obtained with 0.5 mol%, though with a better signal-to-noise. The lipid/chloroform solutions, with or without the fluorescent probe, were dried under a stream of ultrapure N_2, and left under reduced pressure for a minimum of 3 h to remove all traces of organic solvent. Lipid vesicles were prepared by the addition of the 10 mM HEPES solution at pH 7.4, to a final lipid concentration of 1 mM. The samples were heated for 30 min at 60 °C and vortexed every 10 min. The vesicles were extruded 23 times through polycarbonate filters (100 nm pore) at a temperature above the lipid phase transition in order to yield unilamellar vesicles with a maximum diameter of ˜100 nm, checked by Dynamic Light Scattering (100 ± 10 nm). Lipid dispersions were used immediately after preparation.

2.3. Absorbance measurements

Absorbance measurements of DPPC and DODAB vesicles, in the presence and absence of Laurdan, were performed with a Varian Cary 50 UV/Visible spectrophotometer, from 20 °C to 60 °C, with 5 °C intervals, controlled by a Peltier system with ± 0.1 °C precision. Samples were placed in quartz cuvettes sized 4 mm x 10 mm and Absorbance was measured along the 10 mm pathway.

2.4. Steady-state fluorescence measurements

A Varian Cary Eclipse fluorescence spectrophotometer was used for Laurdan steady-state (static) fluorescence intensity and anisotropy measurements, in DPPC and DODAB vesicles. Samples were placed in quartz cuvettes sized 4 mm x 10 mm with the incident beam parallel to the 4 mm pathway. The steady-state fluorescence experiments were performed: (i) at temperatures from 20 °C to 60 °C with 5 °C intervals, with an excitation wavelength of 380 nm, and (ii) at 20 °C, with excitation wavelengths from 270 nm to 420 nm, with 10 nm intervals. Fluorescence anisotropy measurements were collected exciting the sample at 380 nm, recording emission at 480 nm, with automated polarizers:

$$r = (I_{VV} - GI_{VH})/(I_{VV} + 2GI_{VH}) \quad (2)$$

where r is the anisotropy value, I_{VV} and I_{VH} are the fluorescence intensities with the excitation polarizer at the vertical position, and the emission polarizer at vertical and horizontal positions, respectively, and G is the ratio of the sensitivity of the system for vertically and horizontally polarized light [46]. In the fluorescence and anisotropy measurements, the temperature was controlled with a Peltier system, with ± 0.1 °C precision.

2.4.1. Decomposition as a Sum of Gaussians (DSG)

Laurdan fluorescence spectra were decomposed into Gaussian bands, according to Lucio et al., 2010 [44]. In short, the fluorescence spectrum was transformed from wavelength, I(λ), to wavenumber, I(λ^{-1}), considering that the spectrum is recorded with constant wavelength resolution, not energy [47], so I(λ^{-1}) = λ^2I(λ). Upon spectrum decomposition, the population of molecules relaxing from each excited state was calculated by measuring the area under the corresponding band. All spectra fittings were performed with the software *Origin v7.0*.

2.5. Time-resolved fluorescence measurements

Time-resolved fluorescence measurements were performed using time-correlated single photon counting (TCSPC). The fluorescent decay of Laurdan in DODAB vesicles was recorded at 20 °C and 50 °C, at emission wavelengths from 420 nm to 520 nm, every 10 nm. The excitation was fixed at 290 nm. The excitation pulses were generated by a titanium sapphire Tsunami 3950 laser pumped by a 10 W Millennia Pro model J80, both from Spectra Physics. The pulse repetition was set to 8000 kHz rate, using a Spectra Physics 3980-25 pulse picker. The Tsunami was set to give an output of 870 nm and a third harmonic generator BBO crystal (GWN-23PL Spectra Physics) was used to generate the excitation beam at 290 nm, which was directed to an Edinburgh FL900CDT spectrophotometer. The emitted light was detected at 90° from the excitation beam and the emission wavelength was selected with a monochromator. The photons were counted with a refrigerated Hamamatsu R3809U photomultiplier. The FWHM (Full Width at Half Maximum) of the instrument response function was between 90 ps and 110 ps. Time resolution was 12.2 ps per channel. Sample temperature was controlled with a thermal bath Julabo HP 25. FAST software of Edinburgh Photonics v. 0.5 was used to fit the data to a model of exponential decays as:

$$I(\lambda, t) = \Sigma_i \alpha_i e^{-\frac{t}{\tau_i}} \quad (3)$$

where $I(\lambda,t)$ is the number of photons emitted with a given wavelength λ following a time t after the excitation pulse, τ_i is the lifetime of the i^{th} component of decay and α_i is the respective pre-exponential factor, proportional to the species i population.

Fluorescence intensity decays were analyzed by global analysis. Briefly, for a given sample, the set of lifetime decay profiles measured at different wavelengths was fitted with the same lifetimes, but different pre-exponential factors. The adequacy of the multiexponential decay fitting was judged by inspection of the residues of the fitting and by statistical parameters, such as reduced chi-square (χ^2).

The fraction of each excited state decay was calculated by the equation:

$$f_i(\lambda) = \frac{\alpha_i(\lambda)\,\tau_i}{\Sigma_i \alpha_i(\lambda)\,\tau_i} \quad (4)$$

2.6. Decay Associated Spectrum (DAS)

The spectrum of each Laurdan excited state was recovered using the DAS technique, which uses static and time-resolved measurements. The technique is fundamentally explained by Knutson et al. [48] and by Loefroth [49] and applied to Laurdan by Vequi-Suplicy [45,50]. The DAS for each component was calculated considering the intensity $I(\lambda)$ of the steady-state fluorescent spectrum at a fixed wavelength and the fraction $f_i(\lambda)$ (Eq. 4) of each excited state decay, resulting in:

$$I_i(\lambda) = f_i I(\lambda) \quad (5)$$

2.7. Differential scanning calorimetry

Calorimetric measurements were carried out with a Microcalorimeter (Microcal VP-DSC, Northampton, MA, USA). Samples were heated from 20 °C to 60 °C at a scan rate of 20 °C/h. The sample cell (˜500 µL) was filled with a 1 mM lipid dispersion. Baseline subtractions were performed using the MicroCal Origin software with the additional module for DSC data analysis provided by MicroCal. For all systems used, scans shown here are typical profiles obtained from at least three identically prepared samples.

2.8. Reproducibility

Every experiment was performed at least thrice, except for the time-resolved fluorescence experiments, which were performed twice. Error values account for standard deviations and are presented as error bars when larger than the symbols.

3. Results and discussions

The fluorescent properties of Laurdan in DODAB bilayers, at different temperatures, from the absorption to the decay process, are discussed below. They are compared with the fluorescent properties of Laurdan in bilayers of the zwitterionic phospholipid DPPC. These two lipids undergo gel-fluid phase transition around 40–45 °C. Fig. 2 shows typical DSC profiles obtained with extruded vesicles of the lipids used in the present work.

3.1. Optical absorption

The measured Absorbance values of Laurdan in DODAB vesicles, at different wavelengths and different temperatures, are shown in Fig. 3A. As the Absorbance data are a composition of Laurdan optical absorption and the light scattering of DODAB vesicles, the latter profiles, obtained with pure DODAB vesicles (Fig. 3B), were subtracted from the spectra in Fig. 3A, at the same temperature. Accordingly, Fig. 3C exhibits the

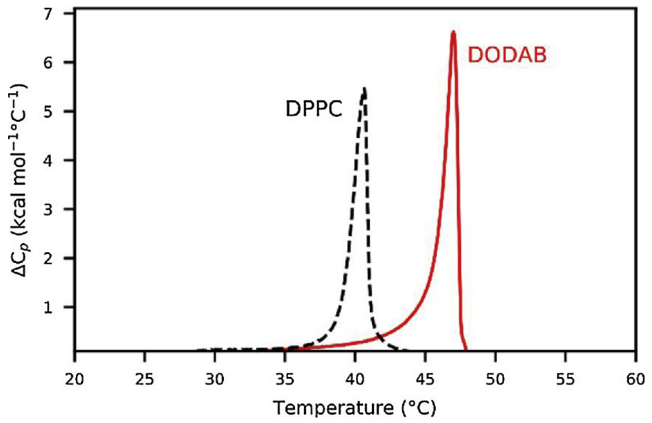

Fig. 2. Typical Differential Scanning Calorimetry (DSC) profiles of 1 mM extruded vesicles (100 nm pores) of DODAB and DPPC. Scans were obtained from 20 °C to 60 °C, with a 20 °C/h scan rate.

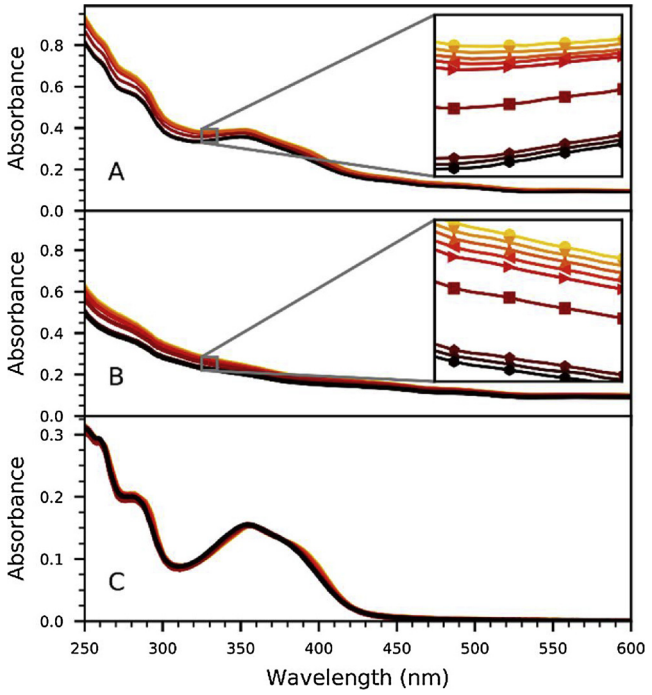

Fig. 3. Absorbance data obtained with Laurdan (10 μM) in DODAB (1 mM) vesicles (A), and with pure DODAB vesicles (B), at different temperatures. Optical absorption spectra of Laurdan in DODAB bilayers (C), obtained from subtracting traces in (A) from those in (B), at the same temperature. Symbols are used for temperature identification only, do not correspond to experimental points: 20 °C, 25 °C, 30 °C, 35 °C, 40 °C, 45 °C, 50 °C, 55 °C, 60 °C. Optical pathway 10 mm.

pure optical absorption spectrum of Laurdan in DODAB bilayers, and evinces its independence of the temperature, from 20 °C to 60 °C, hence its independence of the DODAB bilayer phase (see Fig. 2). These results are similar to those obtained with Laurdan in DPPC bilayers at different temperatures [45]. It is also important to note that the light scattering profiles of DODAB extruded vesicles also do not change significantly with temperature (Fig. 3B), apart from the expected increase in light scattering from the gel to the fluid membrane due to the increase in the size of the lipid vesicles. This illustrates the time and temperature stability of DODAB extruded vesicles used here.

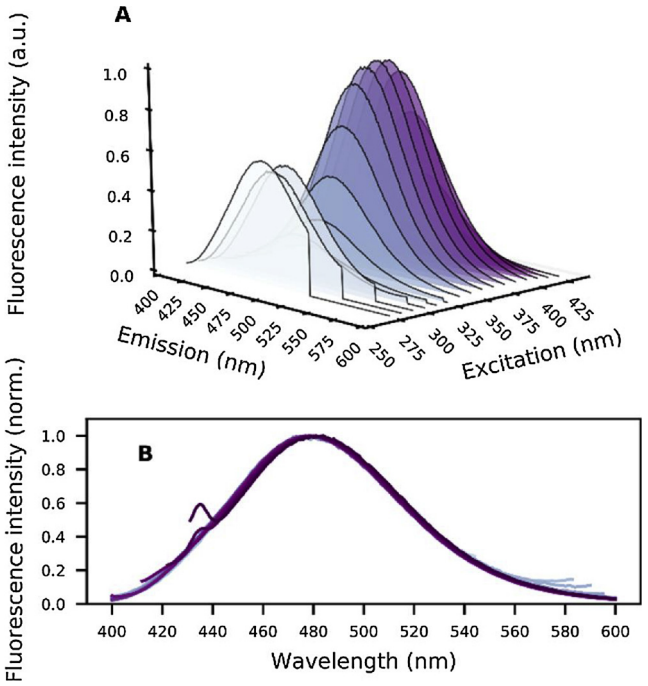

Fig. 4. Set of fluorescent spectra of Laurdan in DODAB vesicles at 20 °C, with varying excitation wavelengths, from 270 nm to 420 nm, with 10 nm intervals (A), and the same spectra normalized (B).

3.2. Steady-state fluorescence

3.2.1. Spectra at different excitation wavelengths

Since the absorption spectrum of Laurdan contains more than one band (Fig. 3C), it is interesting to find out whether the fluorescence spectrum is sensitive to the excitation energy. As expected, the fluorescence intensity is strongly dependent on the excitation wavelength, as shown in Fig. 4A. In DODAB bilayers, Laurdan fluorescence intensity is strong when the probe is excited between 280–290 nm, and even stronger when the probe is excited between 350–380 nm, the latter being the usual excitation range used [1,7]. Apart from the optical properties of Laurdan, the difference in emission intensity could be caused by the different light scattering and/or absorption at the different wavelengths of the incident light that arrives at the centre of the cuvette.

It is important to note that the shape and position of the fluorescence spectra remains unchanged despite the excitation wavelength (Fig. 4B), indicating that the emission is always from the same electronic state or states, independently of the electronic absorption transition. This is quite common for most of the fluorophores, and is known as the Kasha's rule [46].

Given that, we excited the samples at 380 nm in the static fluorescence experiments, to get a better signal to noise ratio. In the time-resolved fluorescence experiments, the 290 nm wavelength was used because the solid-state laser is more intense at smaller wavelengths, balancing the smaller fluorescence intensity of Laurdan and making the time-resolved measurements faster and more reliable.

3.2.2. Temperature dependence of the fluorescence spectrum

The emission spectra of Laurdan in DODAB vesicles, from 20 °C to 60 °C, are shown in Fig. 5A. As expected, the intensity of the emission band decreases as temperature increases [46]. However, the position and the shape of the emission band do not change much with the temperature (Fig. 5B). For comparison, the spectra obtained with Laurdan in DPPC vesicles are shown in Fig. 5C, and after normalization in Fig. 5D, and illustrates the typical behaviour of Laurdan in a phospholipid bilayer.

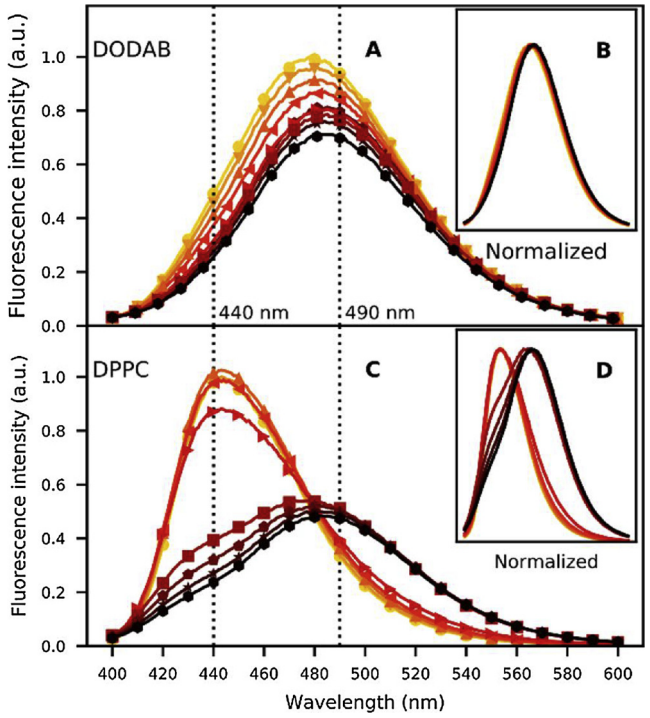

Fig. 5. Fluorescence spectra of Laurdan in DODAB (A and B) and in DPPC (C and D) vesicles at diff ;erent temperatures. (B) and (D) show the spectra of (A) and (C) normalized, respectively. The dashed lines indicate the wavelengths 440 nm and 490 nm, used to calculate the Generalized Polarization. Symbols are used for identification only, do not correspond to experimental points: 20 °C, 25 °C, 30 °C, 35 °C, 40 °C, 45 °C, ▽ 50 °C, △ 55 °C, ▽ 60 °C. λ_{exc} = 380 nm.

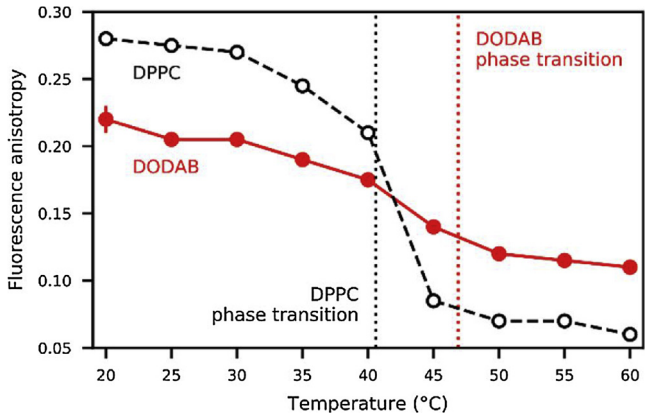

Fig. 6. Steady-state fluorescence anisotropy of Laurdan in DPPC and DODAB vesicles. Symbols correspond to the actual experimental point, and lines are for guiding the eyes only. λ_{exc} = 380 nm.

In DPPC, as in nearly all the phospholipid membranes previously studied [6,44,50,51], Laurdan was found to be very sensitive to the gel-fluid transition of the bilayer. That is known to be related to the strong dependence of the Laurdan emission spectrum on the polarity and viscosity of its environment [6,44], which changes during the thermal phase transition of the membrane. One can see that there is a significant red shift in the Laurdan emission spectrum from the gel to the fluid phase of DPPC, around 41 °C (see Fig. 2). This shift has been used to infer the phase of the membrane by calculating the Generalized Polarization (GP), which is a measurement of the relative intensity of emissions at 440 nm and 490 nm [41]. Although Laurdan has been similarly used in DODAB vesicles for the calculation of the GP [52,53], Fig. 5A and B show that this is not an appropriate parameter, as

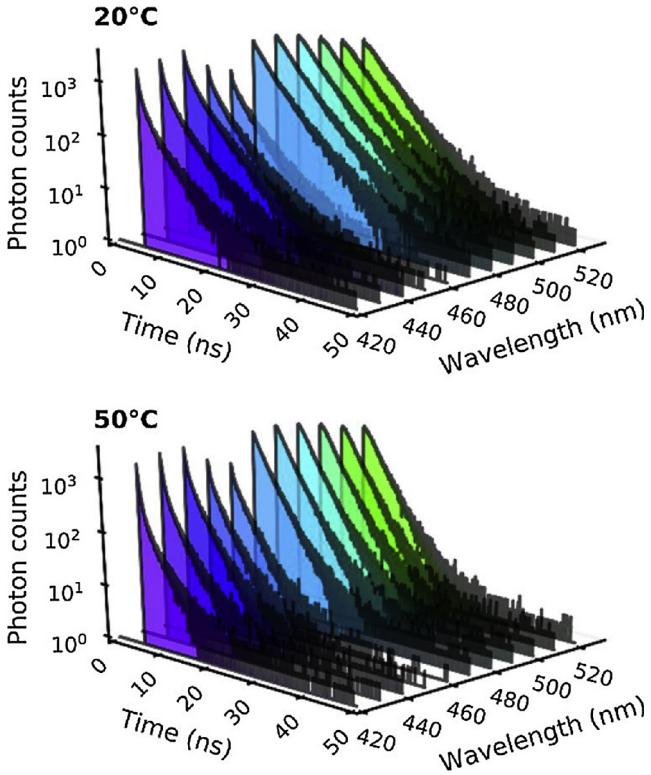

Fig. 7. Fluorescent decays of Laurdan in DODAB membranes, at different wavelengths, in the gel (20 °C) and fluid (50 °C) phases. λ_{exc} = 290 nm.

Table 1
Lifetime values of Laurdan in DODAB and DPPC membranes, before (20 °C) and after (50 °C) the bilayer gel-fluid phase transition. Values in parentheses are the errors in the first decimal position.

	τ_1 (ns)		τ_2 (ns)	
	20°C	50°C	20°C	50°C
DODAB	1.2(6)	0.9(5)	4.1(7)	2.6(1)
DPPC	3.0(3)	2.0(1)	7.1(6)	3.5(1)

Laurdan emission peak in DODAB bilayers nearly does not change with temperature during the phase transition of DODAB, which occurs around 47 °C (see Fig. 2).

Comparing the fluorescence spectra of Laurdan in DODAB and DPPC (Fig. 4), one realizes that the spectra of Laurdan in DODAB, at all temperatures, is more similar to Laurdan in the fluid phase of DPPC (490 nm) than in its gel phase (440 nm). That was the first indication that Laurdan monitors a rather fluid and/or polar environment, both in the gel and fluid phases of DODAB.

3.2.3. *Fluorescence anisotropy*

To gather more information about the fluidity and polarity of the microenvironment of Laurdan in DODAB membranes, we measured the fluorescence anisotropy at different temperatures. The anisotropy is a measurement of how much an excited chromophore rotates before it decays [46]. Hence, it is a balance of the medium viscosity (a viscous medium constrains rotation) and of the excited state lifetime (excited chromophores with longer lifetimes have more time to rotate before decaying). The fluorescence anisotropy is shown in Fig. 6 for Laurdan in DPPC and in DODAB vesicles. For DPPC, there is a clear decrease in the fluorescence anisotropy at the gel-fluid transition around 41 °C, whereas the anisotropy of Laurdan in DODAB decreases constantly with temperature, and there is not a sharp decrease at the gel-fluid transition

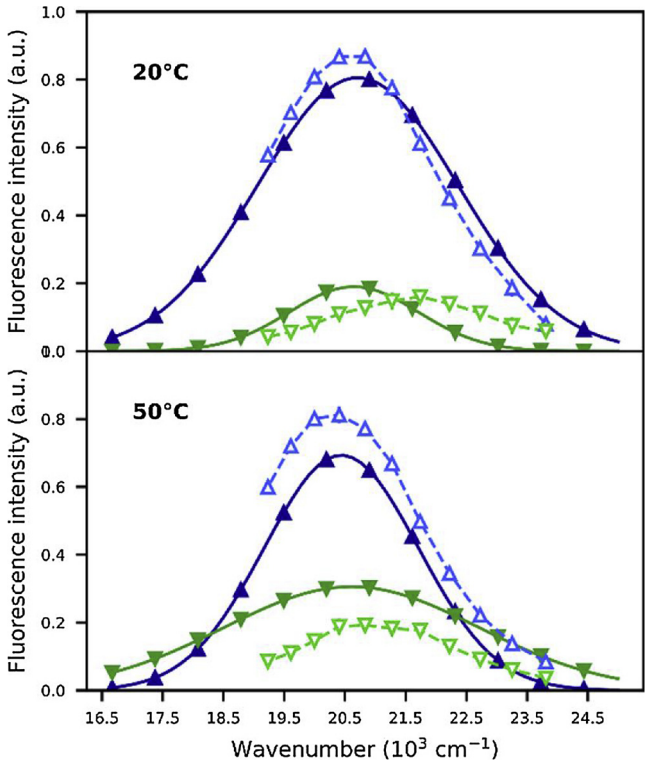

Fig. 8. Spectra decomposition of Laurdan in DODAB. Obtained DAS data are indicated with opened triangles for the shorter (△) and the longer (▼) lifetime decays. Dashed lines are guides for the eyes only. The two Gaussians obtained by the Decomposition of the Spectra as a Sum of Gaussians (DSG) are indicated by the blue — and green — full lines. Full symbols (▲ and ▼—) are used for identification only and do not correspond to experimental points.

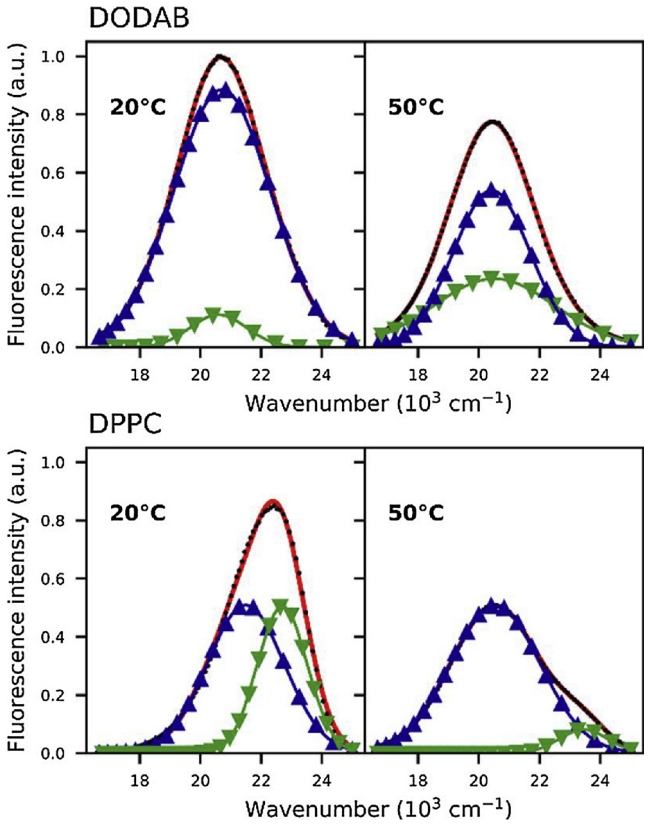

Fig. 9. Decomposition into a sum of two Gaussians (DSG) of the Laurdan emission spectra in DODAB and DPPC, before (20 °C) and after (50 °C) the lipid gel-fluid transition Symbols are used for identification only. Experimental spectrum (…….), Gaussian 1 (—▲—), Gaussian 2 (——), and the sum of the two Gaussian lines (—▼—).

around 47 °C.

As a reference, Prodan, which is a molecule a bit more soluble in water containing the same chromophore as Laurdan, displays a low steady-state fluorescence anisotropy in solution, 0.03, regardless of the temperature [54]. For Laurdan, which is anchored at the lipid bilayer, the anisotropy varies due to the reorganization of the lipid membrane and increasing hydration during phase transition, which modify both the fluidity of the microenvironment and the lifetime of the probe. In the lipid gel phase, the fact that Laurdan in DODAB has an anisotropy smaller than Laurdan in DPPC could indicate that Laurdan in DODAB is in a more fluid environment than in DPPC, at similar temperatures, with an inverse behavior for the lipids in the fluid phase. However, as discussed above, it is important to measure and compare the fluorescent lifetimes of the probe in the two lipids.

3.3. Time resolved fluorescence

The fluorescent decays of Laurdan in DODAB vesicles, at different wavelengths, before (20 °C) and after (50 °C) the gel-fluid phase transition, are displayed in Fig. 7. We observe that the decays are not linear in the semi-log plot. This indicates that the emission is from more than one excited state (see Eq. 3). Using a multiexponential model to fit the set of decays (Global analysis protocol, see Materials and methods), it was possible to fit all data with two exponential decays ($\chi^2 \leq 1.1$), hence two lifetime values, a strong indication that the fluorescent emission of Laurdan in DODAB comes from two excited states, as it has been previously observed for Laurdan in other lipid membranes [6]. Similarly, the fluorescent decays of Laurdan in DPPC vesicles could be well fit with two lifetime values [45]. The found lifetime values, τ_1 and τ_2, for Laurdan in DODAB and DPPC membranes, are shown in Table 1.

As expected, lifetime values decrease significantly as the temperature increases [46]. Both lifetimes, τ_1 and τ_2, are significantly shorter for Laurdan in DODAB than in DPPC bilayers. Shorter lifetimes are associated with higher mobility and/or hydration of the probe, due to the increase of non-radiative relaxation processes, such as collision with water molecules [46]. For instance, the lifetimes for Prodan tumbling freely in water at 20 °C were found to be $\tau_1 = 0.6(1)$ s and $\tau_2 = 2.1(2)$ s [50].

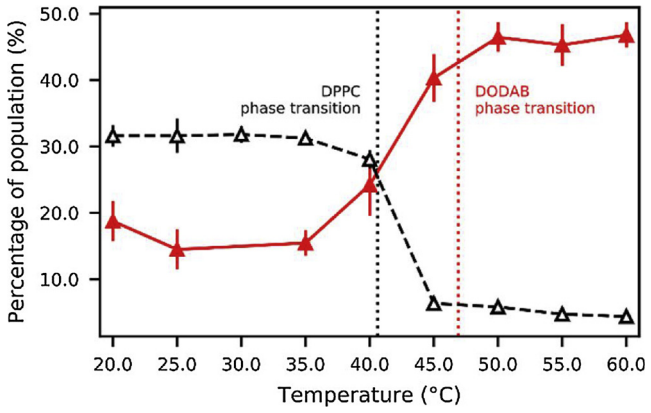

Fig. 10. Percentage of the population (A_1/A_T x100) which displays the shortest lifetime, for Laurdan in DODAB (▲) and in DPPC (△). Symbols correspond to actual experimental points.

Hence, lifetime values indicate that Laurdan in DODAB membranes is in a more hydrated and/or fluid environment than in DPPC, both in the gel and fluid lipid phases, although it is not completely exposed to bulk water like Prodan, as lifetimes are longer than those of Prodan in

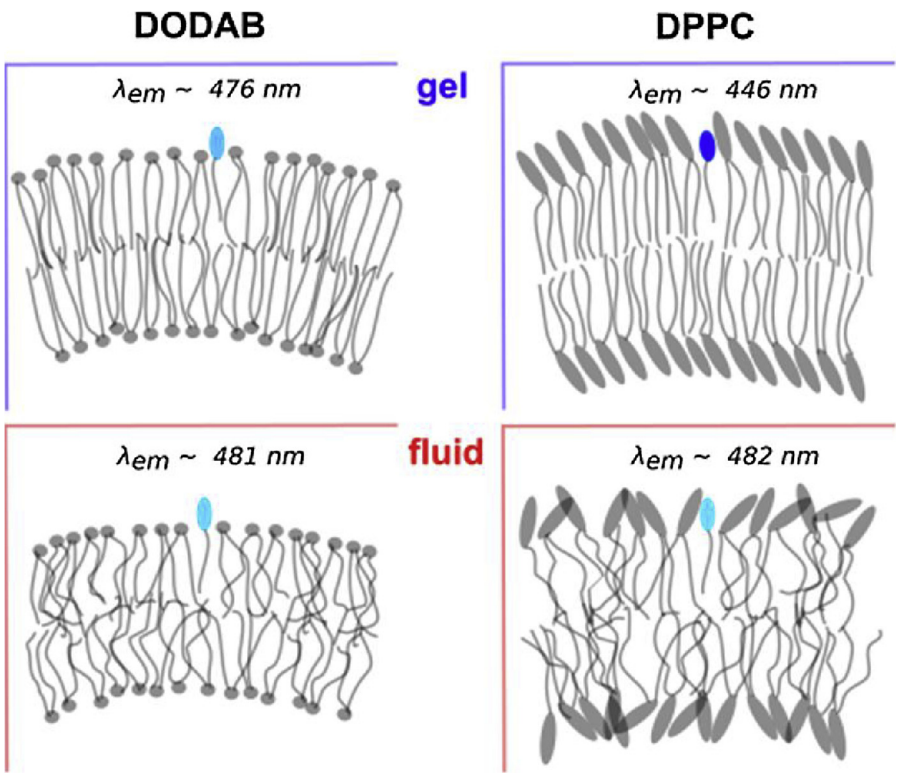

Fig. 11. Models for the position of Laurdan in DODAB and in DPPC bilayers.

water.

As mentioned above, the measured steady state anisotropy will be higher if the lifetime of the excited state is shorter. Hence, shorter lifetimes of Laurdan in DODAB, as compared to DPPC, would lead to higher anisotropy values, even if the mobility of the probe in the two membranes was similar. Therefore, comparing the two lipids, putting together the steady state anisotropy data (Fig. 6) and the calculated lifetime values (Table 1), we have a strong evidence that in gel membranes of DODAB Laurdan monitors a much more fluid/hydrated environment than in DPPC, as in DODAB both the excited state lifetimes (Table 1) and the anisotropy values (see Fig. 6 below 40 °C) are smaller than those obtained in DPPC. In fluid membranes of DODAB and DPPC, anisotropy results are not conclusive, as the excited state lifetimes are shorter in DODAB (Table 1) and the anisotropy values are higher (see Fig. 6 above 45 °C). However, the significantly shorter lifetimes obtained for Laurdan in DODAB, as compared with the probe in DPPC, strongly indicates that the probe is either in a more fluid environment in DODAB and/or in more contact with water molecules.

In the next section, we discuss how phase transition affects the balance of the populations of the two fluorescent excited states of Laurdan.

3.4. Spectrum decomposition

As mentioned above, the need of using two lifetime values to fit the fluorescent decays of Laurdan in DODAB vesicles is a strong indication that Laurdan fluorescence in DODAB comes from two excited states. From lifetime decays at several wavelengths, it is possible to obtain the Decay Associated Spectra (DAS), as described in Materials and methods, which is the calculated emission spectrum of each excited state. Accordingly, Fig. 8 shows the two obtained emission bands of Laurdan, for the shorter (—●—) and longer (—▼—) lifetime decays, in the gel (20 °C) and fluid (50 °C) phases of DODAB bilayer. It is interesting to observe that the fraction of Laurdan molecules decaying from the excited state with shorter lifetime increases as the temperature increases.

Due to the mechanism of fluorescent decay, emission bands are expected to display a Gaussian distribution [46]. Therefore, Laurdan emission spectra in DODAB and DPPC, at different temperatures, were decomposed into Gaussian bands. It was found impossible to well fit the spectra as one Gaussian line only, but two Gaussian lines could well fit the spectra at all temperatures, with $\chi^2 \approx 1$.

Fig. 8 compares the spectral decomposition for Laurdan in DODAB in the gel and fluid phases, with the two methodologies, DAS, which uses the pre-exponential factors obtained with time resolved fluorescence (Eqs. (4) and (5)), and the decomposition of the emission spectrum as a sum of two Gaussian lines (DSG). Fig. 8 shows that the two methodologies yield somehow similar bands, and strengthen the hypothesis of the presence of two emission bands in the Laurdan spectrum in DODAB (similar result was obtained with Laurdan in DPPC).

Because the DSG technique is faster to perform, quite accurate, and the bands coincide reasonably well with those obtained with the DAS methodology, both for Laurdan in DODAB (Fig. 8) and in DPPC (not shown here), we used it to track the populations of excited states at several temperatures. The results of the DSG analysis for Laurdan in DODAB and DPPC, in the gel (20 °C) and fluid (50 °C) phases of the lipids, are compared in Fig. 9.

Gaussian 1 (—▲—), or band 1, corresponds to the excited state which displays the shortest lifetime, as obtained by DAS (see Fig. 8), for both DODAB and DPPC. It is interesting to observe that, for Laurdan in DODAB, the energies of the two bands, 1 and 2, are very similar, whereas for Laurdan in DPPC the energy of the shortest lifetime band, band 1, is clearly higher than that of band 2.

The area under the Gaussian line is proportional to the number of molecules emitting from the corresponding excited state [6,44]. Considering A_1 the area under band 1, the fraction of molecules decaying from band 1 can be calculated as A_1/A_T, where A_T is the total area under the fluorescent spectrum $A_T = A_2 + A_1$. The percentage of the Laurdan population corresponding to band 1 (A_1/A_T x 100) is shown in Fig. 10 for the two lipids, at different temperatures.

Data for Laurdan in DPPC is very similar to that obtained for

Laurdan in DMPG [44]. Namely, at the gel-fluid transition temperature there is a sharp decrease in the population corresponding to the lower lifetime decay (A_1), which corresponds to the fluorescence band with higher energy. That is exactly what makes the fluorescence spectrum of Laurdan in phospholipids so sensitive to the lipid phase transition.

As discussed (Fig. 5), the fluorescence spectrum of Laurdan in DODAB is almost insensitive to the lipid bilayer thermal phase. However, the relative populations of the two excited states do change significantly at the bilayer gel-fluid transition, as shown in Fig. 10. That is explained by the finding that the two Laurdan bands display similar energies for the probe in DODAB, different from what happens with Laurdan in DPPC (Fig. 9). Interestingly, while the population of the lower lifetime band, and higher energy, decreases at the gel-fluid transition for DPPC, it increases for Laurdan in DODAB. That remains to be better understood, possibly with molecular simulation using both classical and quantum approaches.

4. Conclusions

Different from Laurdan in phospholipids, Laurdan in DODAB does not display a significant red shift when the lipid undergoes the gel-fluid transition. Therefore, the largely used methodology for identifying the lipid phase by calculating the Generalized Polarization (GP) from Laurdan fluorescence spectrum is not appropriate for Laurdan in DODAB bilayers. However, using both static and time-resolved fluorescence, it was possible to show that the Laurdan spectrum in DODAB, like in phospholipids, is composed of two different emission bands, associated with two excited states with different lifetimes. The relative intensity of the bands is sensitive to the bilayer thermal phase, and could be used to characterize the DODAB bilayer phase.

The longer wavelength of the maximum of the fluorescence band of Laurdan in the gel phase of DODAB, the lifetimes of the excited states and the lower fluorescence anisotropy (compared to the probe in phospholipids) are strong indications that Laurdan in gel DODAB is much more exposed to water at the bilayer surface than in phospholipids, as illustrated in the sketch on Fig. 11. Even for the fluid phase of the lipids, lower lifetimes (Table 1) indicate more relaxation caused by exposure to water. That could possibly be attributed to the small headgroup of DODAB compared to those of phospholipids.

Therefore, given the shallow position of Laurdan in DODAB membranes, this probe seems to be appropriate for detecting interactions at the bilayer surface. It might be useful, for instance, to characterize the interaction of DODAB with genetic material or other biological relevant molecules [55].

Acknowledgements

This work was supported by FAPESP *via* the project grant 2013/14419-3 and scholarship 2013/24949-0. CCV-S acknowledges fellowship supports also from FAPESP (05/52408-7; 06/55513-9; 10/08365-0). MTL acknowledges fellowship supports from CNPq. And it also has been partially supported by the following Brazilian agencies and projects: CNPq, CAPES, NAP-FCx and INCT-FCx.

References

[1] T. Parasassi, G. De Stasio, G. Ravagnan, R.M. Rusch, E. Gratton, Quantitation of lipid phases in phospholipid vesicles by the generalized polarization of Laurdan fluorescence, Biophys. J. 60 (1991) 179–189, https://doi.org/10.1016/S0006-3495(91)82041-0.

[2] F.M. Harris, K.B. Best, J.D. Bell, Use of laurdan fluorescence intensity and polarization to distinguish between changes in membrane fluidity and phospholipid order, Biochim. Biophys. Acta Biomembr. 1565 (2002) 123–128, https://doi.org/10.1016/S0005-2736(02)00514-X.

[3] S.A. Sanchez, M.A. Tricerri, G. Gunther, E. Gratton, Laurdan Generalized Polarization: from cuvette to microscope, Mod. Res. Educ. Top. Microsc. 2 (2007) 1007–1014.

[4] J. Sýkora, P. Kapusta, V. Fidler, M. Hof, On what time scale does solvent relaxation in phospholipid bilayers happen? Langmuir 18 (2002) 571–574, https://doi.org/10.1021/la011337x.

[5] T. Parasassi, E.K. Krasnowska, L. Bagatolli, E. Gratton, Laurdan and Prodan as polarity-sensitive fluorescent membrane probes, J. Fluoresc. 8 (1998) 365–373, https://doi.org/10.1023/A:1020528716621.

[6] C.C. De Vequi-Suplicy, C.R. Benatti, M.T. Lamy, Laurdan in fluid bilayers: position and structural sensitivity, J. Fluoresc. 16 (2006) 431–439, https://doi.org/10.1007/s10895-005-0059-3.

[7] T. Parasassi, G. Destasio, A. Dubaldo, E. Gratton, Phase fluctuation in phospholipid-membranes revealed by laurdan fluorescence, Biophys. J. 57 (1990) 1179–1186.

[8] M. Viard, J. Gallay, M. Vincent, M. Paternostre, Origin of laurdan sensitivity to the vesicle-to-micelle transition of phospholipid-octylglucoside system: a time-resolved fluorescence study, Biophys. J. 80 (2001) 347–359.

[9] R.M. Epand, B.T.C. Leon, Hexagonal phase forming propensity detected in phospholipid bilayers with fluorescent probes, Biochemistr. 31 (1992) 1550–1554.

[10] A.W. Shaw, M.A. McLean, S.G. Sligar, Phospholipid phase transitions in homogeneous nanometer scale bilayer discs, FEBS Lett. 556 (2004) 260–264, https://doi.org/10.1016/S0014-5793(03)01400-5.

[11] T. Parasassi, G. Ravagnan, R.M. Rusch, E. Gratton, Modulation and dynamics of phase properties in phospholipid mixtures detected by laurdan fluorescence, Photochem. Photobiol. (1993), https://doi.org/10.1111/j.1751-1097.1993.tb02309.x.

[12] O. Golfetto, E. Hinde, E. Gratton, Laurdan fluorescence lifetime discriminates cholesterol content from changes in fluidity in living cell membranes, Biophys. J. 104 (2013) 1238–1247, https://doi.org/10.1016/J.BPJ.2012.12.057.

[13] P. Carravilla, J.L. Nieva, F.M. Goñi, J. Requejo-Isidro, N. Huarte, Two-photon laurdan studies of the ternary lipid mixture DOPC:SM:cholesterol reveal a single liquid phase at Sphingomyelin:cholesterol ratios lower than 1, Langmuir 31 (2015) 2808–2817, https://doi.org/10.1021/la504251u.

[14] A. Ambrosini, G. Bossi, S. Dante, B. Dubini, L. Gobbi, L. Leone, M. Grazia, Ponzi Bossi, G. Zolese, Lipid-drug interaction: thermodynamic and structural effects of antimicotic fluconazole on DPPC liposomes, Chem. Phys. Lipids 95 (1998) 37–47, https://doi.org/10.1016/S0009-3084(98)00062-0.

[15] M. Engelke, P. Bojarski, R. Bloß, H. Diehl, Tamoxifen perturbs lipid bilayer order and permeability: comparison of DSC, fluorescence anisotropy, Laurdan generalized polarization and carboxyfluorescein leakage studies, Biophys. Chem. 90 (2001) 157–173, https://doi.org/10.1016/S0301-4622(01)00139-9.

[16] P.L.-G. Chong, Interctions of laurdan with membranes at high pressures, High Press. Res. 5 (1990) 761–763, https://doi.org/10.1080/08957959008246251.

[17] C. Nicolini, J. Kraineva, M. Khurana, N. Periasamy, S.S. Funari, R. Winter, Temperature and pressure effects on structural and conformational properties of POPC/SM/cholesterol model raft mixtures - a FT-IR, SAXS, DSC, PPC and Laurdan fluorescence spectroscopy study, Biochim. Biophys. Acta-Biomembr. 1758 (2006) 248–258.

[18] C.N.C. Sobral, M.A. Soto, A.M. Carmona-Ribeiro, Characterization of DODAB/DPPC vesicles, Chem. Phys. Lipids 152 (2008) 38–45, https://doi.org/10.1016/J.CHEMPHYSLIP.2007.12.004.

[19] K. Suga, T. Yokoi, D. Kondo, K. Hayashi, S. Morita, Y. Okamoto, T. Shimanouchi, H. Umakoshi, Systematical characterization of phase behaviors and membrane properties of fatty acid/didecyldimethylammonium bromide vesicles, Langmuir 30 (2014) 12721–12728, https://doi.org/10.1021/la503331r.

[20] E. Lemp, A.L. Zanocco, G. Günther, Structural changes in DODAC unilamellar liposomes by addition of sucrose esters monitored by using fluorescent techniques, Colloids Surf. A Physicochem. Eng. Asp. 229 (2003) 63–73, https://doi.org/10.1016/J.COLSURFA.2003.07.001.

[21] M.C. Pedroso De Lima, S. Simões, P. Pires, H. Faneca, N. Düzgüneş, Cationic lipid-DNA complexes in gene delivery: from biophysics to biological applications, Adv. Drug Deliv. Rev. (2001), https://doi.org/10.1016/S0169-409X(01)00110-7.

[22] J. Zabner, A.J. Fasbender, T. Moninger, K.A. Poellinger, M.J. Welsh, Cellular and molecular barriers to gene transfer by a cationic lipid, J. Biol. Chem. 270 (1995) 18997–19007, https://doi.org/10.1074/JBC.270.32.18997.

[23] Y. Barenholz, Liposome application: problems and prospects, Curr. Opin. Colloid Interface Sci. 6 (2001) 66–77, https://doi.org/10.1016/S1359-0294(00)00090-X.

[24] T.M. Allen, P.R. Cullis, Drug delivery systems: entering the mainstream, Science 303 (2004) 1818–1822, https://doi.org/10.1126/science.1095833.

[25] B. Guy, N. Pascal, A. Françon, A. Bonnin, S. Gimenez, E. Lafay-Vialon, E. Trannoy, J. Haensler, Design, characterization and preclinical efficacy of a cationic lipid adjuvant for influenza split vaccine, Vaccine 19 (2001) 1794–1805, https://doi.org/10.1016/S0264-410X(00)00386-8.

[26] G. Hermanson, V. Whitlow, S. Parker, K. Tonsky, D. Rusalov, M. Ferrari, P. Lalor, M. Komai, R. Mere, M. Bell, K. Brenneman, A. Mateczun, T. Evans, D. Kaslow, D. Galloway, P. Hobart, A cationic lipid-formulated plasmid DNA vaccine confers sustained antibody-mediated protection against aerosolized anthrax spores, Proc. Natl. Acad. Sci. 101 (2004) 13601–13606, https://doi.org/10.1073/pnas.0405557101.

[27] A. Schnyder, J. Huwyler, Drug transport to brain with targeted liposomes, NeuroRX 2 (2005) 99–107, https://doi.org/10.1602/neurorx.2.1.99.

[28] J. Kreuter, Nanoparticulate systems for brain delivery of drugs, Adv. Drug Deliv. Rev. 47 (2001) 65–81, https://doi.org/10.1016/S0169-409X(00)00122-8.

[29] R. Koynova, L. Wang, R.C. MacDonald, An intracellular lamellar-nonlamellar phase transition rationalizes the superior performance of some cationic lipid transfection agents, Proc. Natl. Acad. Sci. 103 (2006) 14373–14378, https://doi.org/10.1073/pnas.0603085103.

[30] J. You, M. Kamihira, S. Iijima, Enhancement of transfection efficiency by protamine in DDAB lipid vesicle-mediated gene transfer, J. Biochem. 125 (1999) 1160–1167, https://doi.org/10.1093/oxfordjournals.jbchem.a022399.

[31] J.P.N. Silva, A.C.N. Oliveira, M.P.P.A. Casal, A.C. Gomes, P.J.G. Coutinho, O.P. Coutinho, M.E.C.D.R. Oliveira, DODAB:monoolein-based lipoplexes as non-viral vectors for transfection of mammalian cells, Biochim. Biophys. Acta Biomembr. 1808 (2011) 2440–2449, https://doi.org/10.1016/J.BBAMEM.2011.07.002.

[32] T. Parasassi, M. Di Stefano, M. Loiero, G. Ravagnan, E. Gratton, Influence of cholesterol on phospholipid bilayers phase domains as detected by Laurdan fluorescence, Biophys. J. 66 (1994) 120–132, https://doi.org/10.1016/S0006-3495(94)80763-5.

[33] D. Zubiri, A. Domecq, D.L. Bernik, Phase behavior of phosphatidylglycerol bilayers as a function of buffer composition: fluorescence studies using Laurdan probe, Colloids Surf. B Biointerfaces 13 (1999) 13–28, https://doi.org/10.1016/S0927-7765(98)00106-4.

[34] E.M. Kerek, E.J. Prenner, Inorganic cadmium affects the fluidity and size of phospholipid based liposomes, Biochim. Biophys. Acta Biomembr. 1858 (2016) 3169–3181, https://doi.org/10.1016/J.BBAMEM.2016.10.005.

[35] O. Wesołowska, A.B. Hendrich, N. Motohashi, M. Kawase, P. Dobryszycki, A. Ożyhar, K. Michalak, Presence of anionic phospholipids rules the membrane localization of phenothiazine type multidrug resistance modulator, Biophys. Chem. 109 (2004) 399–412, https://doi.org/10.1016/J.BPC.2003.11.004.

[36] C. Dietrich, L.A. Bagatolli, Z.N. Volovyk, N.L. Thompson, M. Levi, K. Jacobson, E. Gratton, Lipid rafts reconstituted in model membranes, Biophys. J. 80 (2001) 1417–1428, https://doi.org/10.1016/S0006-3495(01)76114-0.

[37] L. Bagatolli, T. Parasassi, E. Gratton, Giant phospholipid vesicles: comparison among the whole lipid sample characteristics using different preparation methods: a two photon fluorescence microscopy study, Chem. Phys. Lipids 105 (2000) 135–147, https://doi.org/10.1016/S0009-3084(00)00118-3.

[38] A.A. Vallejo, J.B. Velázquez, M.S. Fernández, Lateral organization of mixed, two-phosphatidylcholine liposomes as investigated by GPS, the slope of Laurdan generalized polarization spectra, Arch. Biochem. Biophys. 466 (2007) 145–154, https://doi.org/10.1016/J.ABB.2007.06.031.

[39] L.A. Bagatolli, E. Gratton, G.D. Fidelio, Water dynamics in glycosphingolipid aggregates studied by LAURDAN fluorescence, Biophys. J. 75 (1998) 331–341, https://doi.org/10.1016/S0006-3495(98)77517-4.

[40] T. Parasassi, E. Gratton, W.M. Yu, P. Wilson, M. Levi, Two-photon fluorescence microscopy of laurdan generalized polarization domains in model and natural membranes, Biophys. J. 72 (1997) 2413–2429, https://doi.org/10.1016/S0006-3495(97)78887-8.

[41] L.A. Bagatolli, E. Gratton, Two-photon fluorescence microscopy observation of shape changes at the phase transition in Phospholipid Giant Unilamellar Vesicles, Biophys. J. 77 (1999) 2090–2101, https://doi.org/10.1016/S0006-3495(99)77050-5.

[42] M. Viard, J. Gallay, M. Vincent, O. Meyer, B. Robert, M. Paternostre, Laurdan solvatochromism: solvent dielectric relaxation and intramolecular excited-state reaction, Biophys. J. 73 (1997) 2221–2234, https://doi.org/10.1016/S0006-3495(97)78253-5.

[43] K.A. Kozyra, J.R. Heldt, J. Heldt, Influence of spectral heterogeneity of prodan and laurdan solutions on the transfer of electronic energy to octadecyl rhodamine B, Biophys. Chem. 121 (2006) 57–64, https://doi.org/10.1016/J.BPC.2005.11.009.

[44] A.D. Lúcio, C.C. Vequi-Suplicy, R.M. Fernandez, M.T. Lamy, Laurdan Spectrum decomposition as a tool for the analysis of surface bilayer structure and polarity: a study with DMPG, peptides and cholesterol, J. Fluoresc. 20 (2010) 473–482, https://doi.org/10.1007/s10895-009-0569-5.

[45] C.C. Vequi-Suplicy, M.T. Lamy, K. Coutinho, Experimental and Theoretical Studies of the Electronic Spectra of Prodan and Laurdan in Solvents and Lipid Bilayers, Universidade de São Paulo, 2010, https://doi.org/10.11606/T.43.2010.tde-21102010-094046.

[46] J.R. Lakowicz, Principles of Fluorescence Spectroscopy, Springer, 2006, https://doi.org/10.1007/978-0-387-46312-4.

[47] B. Valeur, M.N. Berberan-Santos, Molecular Fluorescence : Principles and Applications, Wiley-VCH, 2013.

[48] J.R. Knutson, D.G. Walbridge, L. Brand, Decay-associated fluorescence-spectra and the heterogeneous emission of alcohol-dehydrogenase, Biochemistry 21 (1982) 4671–4679, https://doi.org/10.1021/bi00262a024.

[49] J.E. Loefroth, Time-resolved emission spectra, decay-associated spectra, and species-associated spectra, J. Phys. Chem. 90 (1986) 1160–1168, https://doi.org/10.1021/j100278a040.

[50] C.C. Vequi-Suplicy, K. Coutinho, M.T. Lamy, New insights on the fluorescent emission spectra of Prodan and laurdan, J. Fluoresc. 25 (2015) 621–629, https://doi.org/10.1007/s10895-015-1545-x.

[51] K.A. Riske, R.P. Barroso, C.C. Vequi-Suplicy, R. Germano, V.B. Henriques, M.T. Lamy, Lipid bilayer pre-transition as the beginning of the melting process, Biochim. Biophys. Acta Biomembr. 1788 (2009) 954–963, https://doi.org/10.1016/J.BBAMEM.2009.01.007.

[52] C.A. Carvalho, C. Olivares-Ortega, M.A. Soto-Arriaza, A.M. Carmona-Ribeiro, Interaction of gramicidin with DPPC/DODAB bilayer fragments, Biochim. Biophys. Acta Biomembr. 1818 (2012) 3064–3071, https://doi.org/10.1016/J.BBAMEM.2012.08.008.

[53] K. Suga, K. Akizaki, H. Umakoshi, Quantitative Monitoring of Microphase Separation Behaviors in Cationic Liposomes Using HHC, DPH, and Laurdan: Estimation of the Local Electrostatic Potentials in Microdomains, Langmuir 32 (2016) 3630–3636, https://doi.org/10.1021/acs.langmuir.5b04682.

[54] C.C. Vequi-Suplicy, K. Coutinho, M. Teresa Lamy, Optical characterization of Prodan aggregates in water medium, Phys. Chem. Chem. Phys. 15 (2013) 11800, https://doi.org/10.1039/c3cp51776d.

[55] J.H.K. Rozenfeld, E.L. Duarte, T.R. Oliveira, M.T. Lamy, Structural insights on biologically relevant cationic membranes by ESR spectroscopy, Biophys. Rev. 9 (2017) 633–647, https://doi.org/10.1007/s12551-017-0304-4.